CHEMICAL ENGINEERING TRANSACTIONS Volume 17, 2009
Editor Sauro Pierucci
 ISBN 978-88-95608-01-3 ISSN 1974-9791
DOI: 10.3303/CET0917145

Ultrafiltration of Food Biopolymers: A Dimensionless Approach to the Generalised Darcy Model Parameters

Mauro Moresi (mmoresi@unitus.it) and Ilio Sebastiani (ilio_seb@yahoo.it)
Department of Food Science and Technology
University of Tuscia, Viterbo, Italy, Tel. n° +39 0761 357498

In this paper, a series of hydraulic tests and experimental trials were performed in a laboratory-scale plant equipped with a ceramic tubular UF membrane module and fed with aqueous solutions of two target food biopolymers (i.e., sodium alginate and citrus pectin) at different feed superficial velocities, solute concentrations and trans-membrane pressure differences (ΔP) in the ranges of 4-6 m s^{-1}, 2.2-30.5 kg m^{-3}, and 0.5-4.2 bar, respectively. The experimental permeation flux (J_P)-vs.-ΔP curves were used to assess the effect of flow conditions on the total resistance to solvent flow (R_T) together with the relative contribution of the membrane resistances due to fouling (R_f) and concentration polarization layer (R_{CP}). Two empiric relationships between the dimensionless polarisation layer resistance index (Φ') and modified Reynolds (Re') and Schmidt (Sc') numbers were also established in the laminar and turbulent flow conditions.

1. Introduction

The permeation flux (J_P) decline observed throughout the ultrafiltration (UF) of highly viscous solutions can be almost entirely attributed to the formation of a polarised and/or cake layer on the membrane surface, as well as blocking of membrane surface pores or fouling of support materials (Cheryan, 1998; Dauphin et al, 1998). To overcome such uncertainties, as well as the lack of reliable design equations, long-term laboratory- and pilot-scale experiments are therefore needed to determine the effects of the main operating parameters (i.e., membrane characteristics, porosity and configuration; feed superficial velocity, v_S, and solute concentration, c_B; transmembrane pressure difference, ΔP; density; pH and temperature) on membrane process performance.
A great number of papers have so far attempted to design or optimise UF units by resorting to the generalized Darcy law or film theory (Cheryan, 1998; Krishna Kumar et al, 2004; Prádanos et al, 1995; Todisco et al, 2002; Yazdanshenas et al, 2005).
In previous work (Moresi and Sebastiani, 2008), a six-step experimental procedure was set up so as to determine the empiric parameters of the film theory to predict the permeation flux in the pressure-independent, mass transfer-controlled region.
The main aim of this work was to apply such a procedure to determine all the parameters of the generalized Darcy law and resort to the dimensional analysis to assess the effect of flow regime on the membrane resistance due to the concentration polarization layer (R_{CP}) and describe the dependence of J_P on ΔP in both pressure- and mass-transfer controlled regions.

Please cite this article as: Moresi M. and Sebastiani I., (2009), Ultrafiltration of food biopolymers: a dimensionless approach to the generalised darcy model parameters, Chemical Engineering Transactions, 17, 867-872 DOI: 10.3303/CET0917145

2. Materials and Methods

Commercial samples of sodium alginate (SA) $[C_6H_7O_6Na]_n$ type LF 10/60 L from *Lessonia nigrescens*, characterised by 60% of mannuronic residues and kindly provided by Claudio Savini & Figli S.r.l. (Milan, I), or citrus pectin (CP) (Sigma, EC n° 232-553-0, batch n° 900-69-5), characterised by a galacturonic acid content of 93.5% with a degree of methyl esterification (DE) of 63-66% and a methoxy content of 9.4%, were dissolved in 0.1 kmol m^{-3} NaCl.

A typical temperature- and pressure-controlled bench-top UF plant, previously described (Moresi and Sebastiani, 2008) was used. It was equipped with a tubular, 20 kDa NMWCO α-alumina UF membrane module, provided by US Filter (Warrendale, PA, USA), with 6-mm inside diameter (d), 500-mm length, and 94.2-cm^2 effective membrane surface area. The stainless steel centrifugal pump (type HMS, Lowara, Montecchio Maggiore, Italy) was piloted using a 0.75 kW electric motor via a frequency inverter Commander SK (Control Techniques, Powys, UK) so as to vary ΔP under constant v_S. The process temperature was monitored and automatically controlled by an on-off temperature-controller. A digital flowmeter transducer (TF) was used to measure the retentate flow rate (0.2-0.9 $m^3 h^{-1}$).

A series of total recycle runs was carried out under different c_B, v_S and ΔP values in the ranges of 2.2-30.5 kg m^{-3}, 4-6 m s^{-1} and 0.5-4.2 bar, respectively, and T=50.0±0.5°C. By using a technical-grade scale (B), type Europe 4000 AR (Gibertini, Elettronica Srl, Novate, Milan, I), interfaced to a personal computer (PC) via a RS-232 serial port, it was possible to estimate the permeation flux (J_P). A few validation tests were carried out in the batch mode at v_S=5 or 6 m s^{-1}, $\Delta P \approx 3$ bar, T=50±0.5°C. The SA or CP concentration in both permeate (c_{BP}) and retentate (c_{BR}) samples was spectrophotometrically determined at 210 or 285 nm by using 1-cm quartz cuvettes, respectively.

3. Results and discussion

In accordance with Cheryan (1998), the effect of transmembrane pressure difference (ΔP) on the solvent permeation flux (J_P) was modelled by means of the conventional filtration or generalized Darcy law:

$$J_P = \Delta P/[\eta_P (R_m + R_f + R_{CP})] \quad (1)$$

where η_P is the permeate viscosity; R_m the intrinsic membrane resistance while R_f and R_{CP} are the membrane resistances due to fouling and the concentration polarization layer, respectively. In particular, the term R_f includes both reversible ($R_{f,rev}$) and irreversible ($R_{f,irrev}$) fouling, the two components being distinguishable by the fact that the permeation flux either can or cannot be recovered after membrane cleaning. For the alginate solutions under study, irreversible fouling was previously observed when using organic spiral-wound modules (Moresi *et al*, 2006).

Before assessing the effect of ΔP on J_P, the membrane module was thoroughly cleaned and, for any trial, ΔP was step by step increased from 0.5-0.7 bar to 4.1-4.2 bar to determine the experimental J_P-*vs*.-ΔP curves. Then, for any concentration and feed superficial velocity tested, the feed was kept recirculating through the membrane module for a couple of hours to assess its stability. Within such a time interval, the maximum variation in J_P was less than 5%, thus indicating that the system had reached steady state. Fig. 1 shows the typical effect of ΔP on J_P for a SA or CP dispersion under constant c_{BR}, as well as the pressure- and mass transfer-controlled regions.

To assess the reproducibility of such permeation tests, the efficiency of the cleaning

procedure for the membrane module of concern was checked by performing sequential water permeation tests for longer than a year and a half. The resulting intrinsic membrane resistance of this laboratory-scale membrane module was practically constant: $R_m=(0.24\pm0.04)\times10^{13}$ m^{-1}.

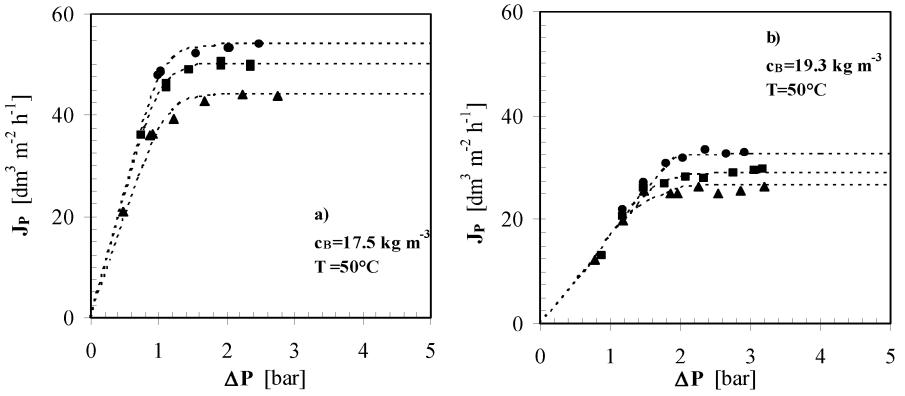

Figure 1 Recovery of sodium alginate (**a**) or citrus pectin (**b**) by UF in the total recycle mode: effect of transmembrane pressure difference (ΔP) on permeation flux (J_P) under constant solute concentration (c_B) and temperature (T) and different feed superficial velocities (v_S: ▲, 4; ■, 5; ●, 6 m s^{-1}).

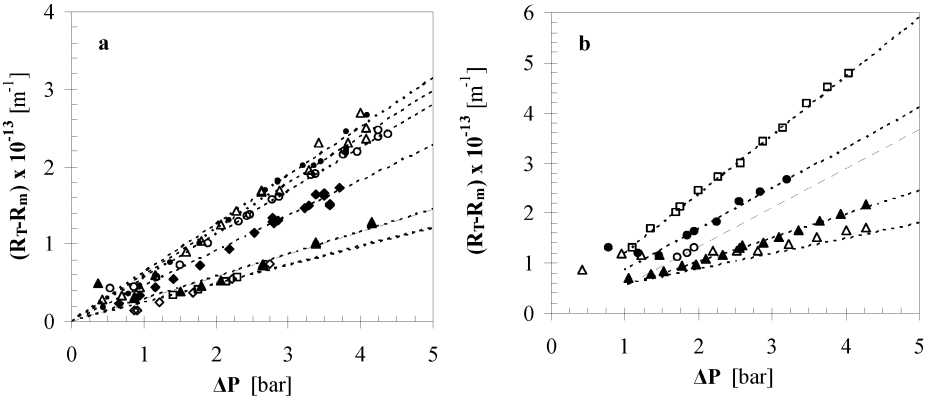

Figure 2 Effect of transmembrane pressure difference (ΔP) on the difference between the overall (R_T) and intrinsic membrane (R_m) resistances at different SA (**a**: ▲, 3.1; ○, 5.2; △, 7.1; ●, 8.3; ◆, 13.1; ◇, 17.5; □, 21.8 kg m^{-3}) or CP (**b**: △, 2.2; ▲, 4.8; □, 9.8; ●, 19.3; ○, 30.4 kg m^{-3}) concentrations and constant feed superficial velocity of 4 m s^{-1}.

In particular, by assuming that R_{CP} is a linear function of ΔP via a proportionality coefficient Φ, called the *polarization layer resistance index* (Masciola *et al*, 2001), the difference between the experimental values of the total resistance to solvent flow [$R_T=\Delta P/(\eta_P J_P)$] and the average value of R_m was plotted against ΔP for all values of c_{BR} and v_S tested, so to assess the contribution of reversible and/or irreversible membrane fouling to the performance of the total recycle UF recovery processes (Fig. 2).

It can be noted that the resistance due to fouling (R_f) was practically nil in all trials concerning the recovery of SA by UF, but it was definitively greater than zero when dealing with CP solutions.

Thus, during the UF of SA solutions the permeation flux decline was of the reversible type, whereas in the case of CP solutions such a decline was only partly reversible, in agreement with Pritchard *et al* (1995), who compared the J_P values in a tubular membrane module fed sequentially with solutions containing pectin or xanthan gum. In all probability, the pectin molecules transported by the solvent permeation flux gave rise not only to a concentration polarization layer, that is reversible by definition, but also to a real gel layer deposited onto the membrane surface.

By plotting Φ against the feed superficial velocity (v_S) in the tubular membrane module, it was noted that Φ tended to decrease as v_S was increased whatever the solute or its concentration (data not shown). However, at v_S=const Φ increased with c_{BR} up to a critical value (c_{BR}*), after that Φ started to decrease. A similar behaviour was also observed by Pritchard *et al* (1995) when assessing the change in J_P related to the transition from turbulent to laminar regime in a tubular UF membrane module fed with CP or xanthan gum aqueous solutions.

Use of dimensional analysis yielded the following dimensionless relationship between Φ and the basic variables affecting the solute mass transfer coefficient in the liquid bulk, that is retentate density (ρ_R) and effective viscosity (η_{Re}), solute diffusivity (D_B), feed superficial velocity (v_S), and tubular module diameter (d):

$$\Phi' = \frac{\Phi\,\eta_{Re}^2}{d\,\rho_R} = \alpha\left(\frac{\rho_R D_B}{\eta_{Re}}\right)^{\beta}\left(\frac{d\,\rho_R v_S}{\eta_{Re}}\right)^{\gamma} = \alpha\,(Sc')^{\beta}(Re')^{\gamma} \qquad (2)$$

where Φ' is the dimensionless polarization layer resistance index, Sc' and Re' are the modified Reynolds and Schmidt numbers, to account for the non-Newtonian behaviour of the SA and CP solutions (Moresi et al., 2008; Moresi and Sebastiani, 2008).

Fig. 3 shows the effect of Re' on the dimensionless ratio $(\Phi')/(Sc')^{1/3}$ as extracted from the total recycle UF tests in the laboratory-scale plant using SA or CP aqueous solutions.

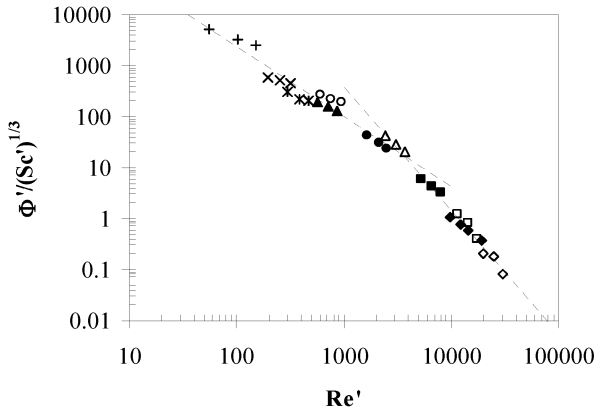

Figure 3 Effect of modified Reynolds number (Re') on $(\Phi')/(Sc')^{1/3}$ as referred to the total recycle mode UF tests at 50°C using different SA or CP concentrations (SA: ◆, 3.1; ■, 5.2; ●, 8.3; ▲, 13.1; ✳, 17.5; ×, 21.8 kg m^{-3}; CP: ◇, 2.2; □, 4.8; △, 9.8; ○, 19.3; +, 30.4 kg m^{-3}).

Data fitting by the least squares method yielded the following two empiric relationships:

$$\Phi'/(Sc')^{1/3} = \begin{cases} e^{14.0\pm0.4}\,(Re')^{-1.37\pm0.06} & (r^2=0.96) \quad \text{for } Re'<3600 \\ e^{22.6\pm0.9}\,(Re')^{-2.4\pm0.1} & (r^2=0.98) \quad \text{per } Re'>3600 \end{cases} \qquad (3)$$

which were used to plot the broken lines in Fig. 3, these intersecting at a critical Re' value of about 3,600. Despite the scatter in the observed $\Phi'/(Sc')^{1/3}$ values (mean percentage error of 22.8%), such an intersection is in line with the general rule that pseudoplastic fluids undergo the transition from laminar to turbulent flow at Re' greater than 2,100 (Dodge and Metzner, 1959).

Fig. 4 shows the time course of two independent validation tests, performed in the batch mode under constant ΔP, v_S and T, using two different feed solution containing SA or CP.

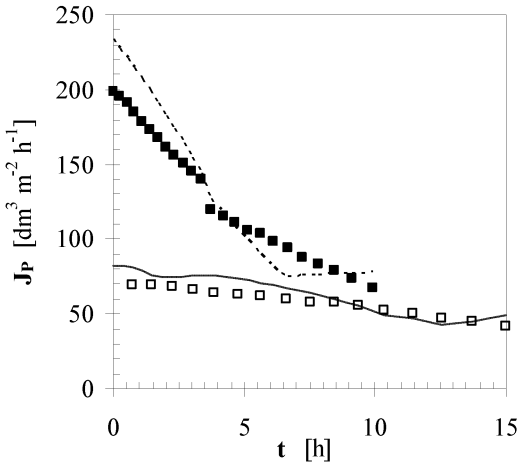

Figure 4 Time course of the permeation flux (J_P) observed during the UF recovery of SA (closed symbols and broken line) or CP (open symbols and continuous line) by the batch mode under constant ΔP, v_S and T (■, SA: c_{B0}= 2.9 kg m^{-3}, v_S=6 m s^{-1}, ΔP=3.0 bar; □, CP: c_{B0}= 4.8 kg m^{-3}, v_S=5 m s^{-1}, ΔP=3.1 bar). Eq.s (1) and (3) together with the R_m and R_f values given in the text were used to plot the continuous and broken lines.

By using the average values of R_m (=0.24x10^{13} m^{-1}) and R_f (=0 for SA, or 0.8x10^{13} m^{-1} for CP) previously estimated and predicting the polarization layer resistance index (Φ) via Eq. (3) as a function of Re' and Sc', it was possible to calculate the instantaneous solvent permeation flux (J_P) via Eq. (1), as shown by the continuous and broken lines plotted in Fig. 4 for CP and SA, respectively.

It is worth noting that the operation for both validation tests started in the turbulent flow regime (with Re' of the order of 15,000), but ended in the laminar one (with Re' in the range of 1,500-1860).

Figure 4 shows that both tests were accurately reconstructed, the average percentage errors between the experimental and calculated permeation fluxes being smaller than 12%.

4. Conclusions

By using a laboratory-scale UF plant, equipped with a ceramic tubular membrane module and a centrifugal pump driven via an asynchronous motor piloted by a frequency inverter to control simultaneously the feed flow rate and input pressure, it was possible to assess the effects of transmembrane pressure difference (ΔP), feed superficial velocity (v_S) and solute concentration (c_{BR}) in the ranges of 0.4-4.2 bar, 4-6 m s^{-1}, and 2.2-30.4 kg m^{-3}, respectively, on the permeation flux under a constant process temperature of 50°C.

The experimental permeation flux (J_P)-vs.-ΔP curves were used to assess the effect of flow conditions on the total resistance to solvent flow (R_T) together with the relative contribution of the membrane resistances due to fouling (R_f) and concentration polarization layer (R_{CP}).

By resorting to two dimensionless empirical regressions among the dimensionless polarisation layer resistance index (Φ') and modified Reynolds (Re') and Schmidt (Sc') numbers valid in the laminar or turbulent flow regime, it was possible to simulate satisfactorily two independent validation tests performed in the batch mode.

Thus, preliminary assessment of R_m and R_f in a laboratory-scale plant together with a rough estimates of RCP, as well as their changes throughout the UF process, may help to design or optimise industrial-scale UF units whatever the trans-membrane pressure difference applied .

5. References

Cheryan M (1998) *Ultrafiltration and Microfiltration Handbook*, Technomic Publ. Co., Lancaster (USA).

Dauphin G, René F, Aimar P (1998) *Les séparations par membrane dans les procédés de l'industrie alimentaire*. Technique & Documentation Lavoisier, Paris.

Dodge DW, Metzner AB (1959) *AIChEJ* **5**: 189-209.

Krishna Kumar NS, Yea MK, Cheryan M (2004) *J Membr Sci* **244**: 235-242.

Masciola DA, Videro RC, Jr, Reed BE (2001) *J Membr Sci* **184**: 197-208.

Moresi M, Ceccantoni B, Lo Presti S, Sebastiani I (2006) Recupero di alginati algali da soluzioni modello mediante ultrafiltrazione, in S. Porretta (Ed.), *Ricerche e innovazioni nell'industria alimentare*. Vol. 7, Chiriotti Editori, Pinerolo (Italy), pp. 183-188.

Moresi M, Sebastiani I (2008) *J Membr Sci* **322:** 349-359.

Moresi M, Sebastiani I, Wiley DE (2008) Experimental Strategy to Assess the Main Engineering Parameters Characterizing Sodium Alginate Recovery from Model Solutions by Ceramic Tubular Ultrafiltration Membrane Modules. *J Membr Sci*, in press.

Prádanos P, de Abajo J, de la Campa JG, Hernández A (1995) *J Membr Sci* **108**: 129-142.

Pritchard M, Field R, Howell JA (1995) *J Membr Sci* **102**: 223-235.

Todisco S, Tallarico P, Gupta BB (2002) *Innovative Food Sci Emerg Technol* **3**: 255-262.

Yazdanshenas M, Tabatabaeenezhad AR, Roostaazad R, Khoshfetrat AB (2005) *Sep Purif Technol* **47**: 52-57.